J Bone Miner Metab (2009) 27:272–286
DOI 10.1007/s00774-009-0038-x

ORIGINAL ARTICLE

Analyses of early events during chondrogenic repair in rat full-thickness articular cartilage defects

Yoshihisa Anraku · Hiroshi Mizuta · Akira Sei · Satoshi Kudo · Eiichi Nakamura · Kei Senba · Yuji Hiraki

Received: 19 December 2007 / Accepted: 17 July 2008 / Published online: 13 February 2009

Abstract In this study we investigated the cellular events that occur during the onset of chondrogenic differentiation during the repair of full-thickness defects of articular cartilage. The V-shaped full-thickness cartilage defects (width 0.7 or 1.5 mm; depth 0.8 mm; length 4 mm) were created in the femoral patellar groove of rats using a custom-built twin-blade device. The time course of the repair response in these cartilage defects was examined using a semi-quantitative histological grading scale. Cartilaginous repair responses failed to occur in the larger 1.5 mm defects, which was covered only by fibrous scar tissue. In contrast, hyaline-like articular cartilage was regenerated concomitantly with the repair of the subchondral bone by 4 weeks in smaller 0.7 mm width defects. Cells in the reparative regions were then characterized by immunohistochemistry and in situ hybridization. Undifferentiated mesenchymal cells migrate into the defects and fill the cavities within 4 days of their creation. The expression of PCNA, N-cadherin, and PTH/PTHrP receptors was induced in cells at the center of the defects, where type II collagen-positive polygonal-shaped cells also begin to appear at day 7. Marrow-derived mesenchymal cells acquire higher levels of proliferative activity in induced cartilage cavities after their initial migration and filling of the smaller 0.7 mm defects. During the regenerative repair of articular cartilage in the rat, there is a distinctive step that appears to be analogous to the precartilaginous condensation that is pivotal during chondrogenesis in development.

Keywords Rat articular cartilage · Full-thickness defects · Chondrogenesis · Tissue repair · Cell condensation

Y. Anraku · H. Mizuta · A. Sei · S. Kudo · E. Nakamura · K. Senba
Department of Orthopaedic and Neuro-Musculoskeletal Surgery, Faculty of Medical and Pharmaceutical Sciences, Kumamoto University, Kumamoto, Japan

Y. Hiraki (✉)
Department of Cellular Differentiation, Institute for Frontier Medical Sciences, Kyoto University, Kyoto 606-8507, Japan
e-mail: hiraki@frontier.kyoto-u.ac.jp

Introduction

Articular cartilage has only a limited regenerative capability, and in partial-thickness defects that are limited to the layer of articular cartilage, no effective repair response occurs [1, 2]. Full-thickness articular cartilage defects that penetrate through the cartilage do undergo regenerative repair of hyaline cartilage under restricted conditions [3, 4]. Marrow-derived mesenchymal cells are considered to be principally responsible for the reparative responses of animals. The lineage progression of mesenchymal cells during repair is influenced by various factors such as the size [3, 5] and location of the defects [1, 6], and also the age [7] of the subject.

In previous studies from our laboratory [8, 9], we have reported on the processes underlying the regenerative repair of articular cartilage with the use of full-thickness articular cartilage defects created in the femoral trochlea of adolescent rabbits as our model. In these analyses, smaller 3 mm cylindrical defects, which show spontaneous regeneration of the surface articular cartilage, were compared with larger 5 mm cavities that fail to undergo chondrogenesis but result in the formation of fibrous scar tissue [5, 8]. For the successful induction of cartilage in these defects, the migration and accumulation of proliferating

mesenchymal cells was found to be critically important at the early stages of the repair process [10, 11].

Rat models of experimentally induced articular cartilage defects have been used to examine cartilage repair. Several authors used larger cylindrical full-thickness defects as control defects [12–14], which were resurfaced with non-cartilaginous tissue. Although this drilling method is suitable for creating defects of a uniform size, it has difficulty in getting enough amounts of sections of the reparative tissue, particularly in the case of the small defects that can spontaneously regenerate rat articular cartilage. Such studies require establishment of an experimental model in rats, which reproduce spatio-temporal events sequentially leading to regenerative repair of articular cartilage and provide enough amounts of sections of reparative tissue. In contrast, V-shaped full-thickness defects have the advantage of providing sufficient sections of reparative tissue [15]. However, it has been relatively difficult to create defects of a uniform size in this way. Thus, we previously developed a rat model containing identically sized V-shaped full-thickness defects of articular cartilage that can undergo chondrogenic repair in a reproducible fashion by the use of a custom-built twin-blade device [16]. In present study, we have utilized immunohistochemistry and in situ hybridization to investigate the cellular events that occur at the onset of chondrogenic differentiation during the repair of cartilage defects using our rat model.

Materials and methods

Creation of full-thickness defects of articular cartilage

A total of 150 6-week-old male Wistar rats, weighing between 140 and 150 g, were utilized in this study. The rats were anesthetized by an intra-abdominal administration of sodium pentobarbital at 30-mg/kg-body weight. The left knee joint was entered through a medial parapatellar incision, and the patella was dislocated laterally to expose the articular surface of the femoral trochlea.

Full-thickness defects of articular cartilage were then created using the twin blade device that could create a precisely defined full-thickness defect of articular cartilage in rats (Fig. 1a, b). To create smaller and larger defects uniformly, two devices with slits of differing lengths and angles were prepared. The desired widths were 0.7 and 1.5 mm and the desired depth and lengths were 0.8 and 4 mm, for the smaller (Fig. 1c, e) and larger (Fig. 1d, f) defects, respectively. Smaller defects were created in 102 of the animal cohort. After the defects were generated, the articular capsule and skin were closed independently with 5–0 nylon sutures. All animals were then allowed to walk freely without splintage. Our research protocol was approved by the animal ethics committee of Kumamoto University School of Medicine, and animal care and experimental procedures were conducted in accordance with institutional guidelines (http://card.medic.kumamoto-u.ac.jp/card/japanese/kisoku/kisoku.html).

Histological analysis of reparative tissues

Groups of ten animals were killed with an overdose of sodium pentobarbital at 2, 4, 7, and 10 days, and at 2, 4, 8, 12, and 24 weeks after the creation of the smaller defects. And groups of six animals were killed at 2, 4, 7, and 10 days and 2 and 4 weeks after generating the larger defects. For subsequent in situ hybridization analysis, samples were prepared under RNase-free conditions. The distal ends of the femurs were fixed overnight in 4% paraformaldehyde in a phosphate buffer saline (pH 7.4), decalcified with 10% EDTA for about 2 weeks at 4°C, and were then embedded in paraffin. Serial sections (5 μm thick) were cut in a transverse plane and stained with safranin-O to examine the sequential repair process in each group. For semi-quantitative analysis of reparative tissue, the sections were examined independently by two observers and were scored according to the semi-quantitative histological grading scale previously described by Pineda et al. with some modifications (Table 1) [17]. The scale that we used is the inverse of the original so that a better recovery of articular structure has a higher score; ranging from 0 (worst) to 14 (best) [18].

Immunohistochemical analysis

For immunostaining analysis, serial sections (5 μm) of the reparative tissue were prepared at 2, 4, 7, and 10 days, and 2, 4, 8, 12, and 24 weeks after creation of smaller full-thickness defects. We first stained the sections with safranin-O, and semiserial sections were then used for immunostaining. Endogenous peroxidase activity was blocked with 0.5% hydrogen peroxide in methanol and the samples were then washed three times in 0.1% bovine serum albumin (BSA) in Tris buffered saline (TBS) for 5 min. The sections then were treated with 500 U/ml testicular hyaluronidase (Sigma Chemical, St Louis, MO, USA). After nonspecific staining was reduced by incubation with horse or goat serum for 30 min, the primary antibodies were applied: a polyclonal antibody against human N-cadherin, incubated overnight at 4°C (dilution 1:400; Santa-Cruz Inc., Santa Cruz, USA); a polyclonal antibody against rat parathyroid hormone (PTH)/PTH-related protein (PTHrP) receptors, incubated overnight at 4°C (dilution 1:400; Babco, Richmond, CA, USA); a polyclonal antibody against human Sox9, incubated

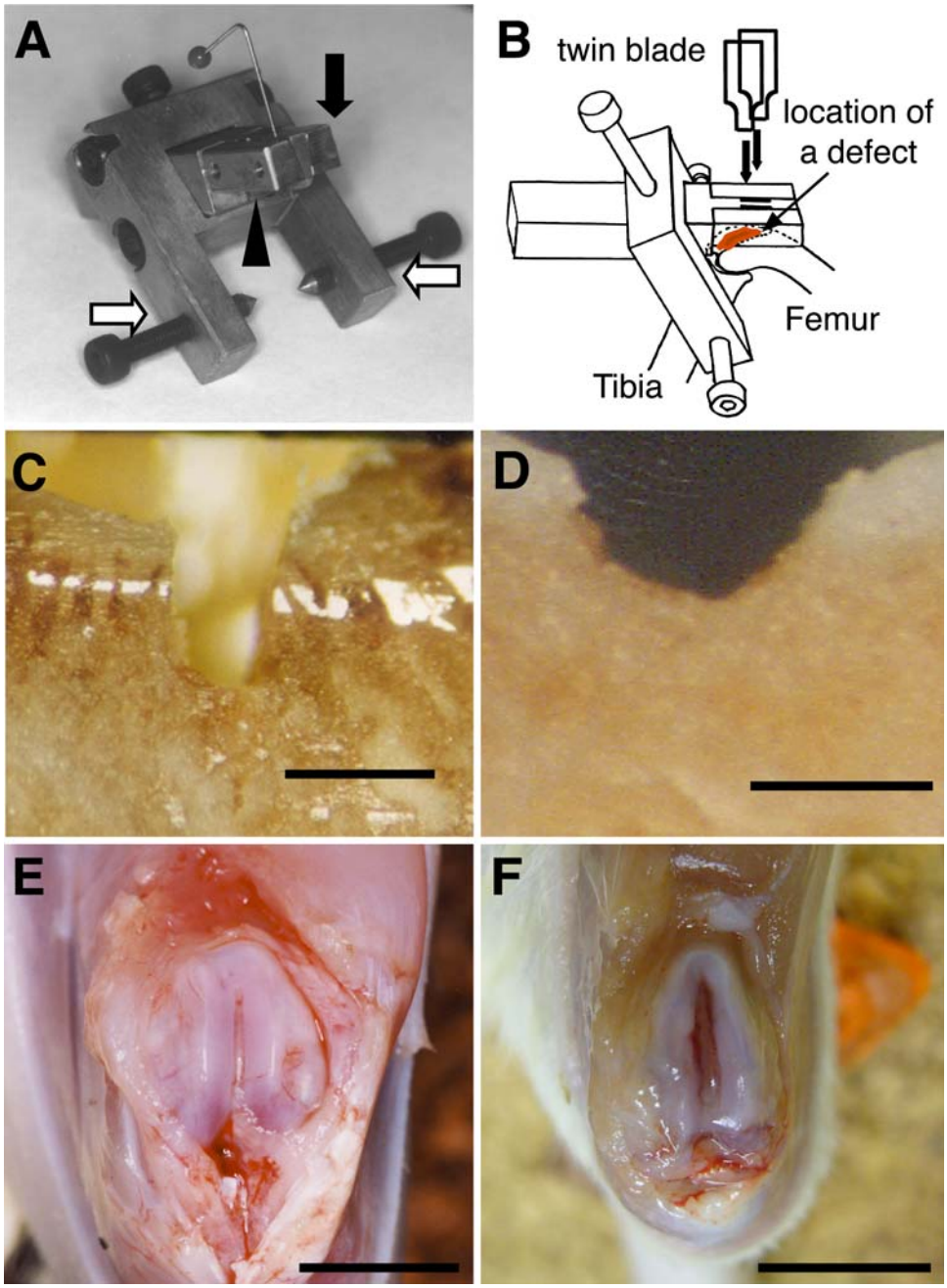

Fig. 1 A custom built twin-blade device for creating full-thickness defects in rat articular cartilage. **a** The device consists of two components: (1) The trunk (*arrow*), which has two slits to enable the twin blades to pass through uniformly, and the contact point of the slit is curved (*arrowhead*) to fit along the femoral patellar groove. (2) The fixator (*open arrows*) which has two screws that anchor the tibia and contains a hexagonal bolt that attaches the two components. **b** Schematic diagram of the twin-blade device fixed to a rat at a 90° knee flexion. **c**, **d** This custom device reproducibly creates both smaller (**c**) and larger (**d**) defects on the rat articular surface of the femoral trochlea. *Bar* 1 mm. **e**, **f** Gross appearance of the defects at 1 week post-injury are shown. **e**, **f** show the smaller 0.7 mm defects and larger 1.5 mm defects, respectively. *Bar* 5 mm

overnight at 4°C (dilution 1:400; Chemicon, CA, USA) [19]; a polyclonal antibody against human Runx2, incubated overnight at 4°C (dilution 1:400; Santa-Cruz, CA, USA) [20]; a monoclonal antibody against human type II collagen, incubated overnight at 4°C (dilution 1:100; Fuji Chemical, Takaoka, Japan); a monoclonal antibody against proliferating cell nuclear antigen (PCNA), incubated 1 h at room temperature (dilution 1:400; Dakopatts, Copenhagen, Denmark). Subsequent reactions were performed using a Vectastain avidin–biotin peroxidase complex (ABC) kit (Vector Laboratories, Burlingame, CA, USA). After three washes with TBS for 5 min each, biotinylated secondary antibodies and avidin–biotin peroxidase complexes were applied in a humid chamber. The sections were then reacted with a 3,3-diaminobenzidine (DAB) solution and counterstained in 0.5% Mayer's hematoxylin. The specificity and cross-reactivities of the antibodies to rat N-cadherin were examined using rat bones [21] and brains [22] as a positive control and rat tongues and small intestines [23] as a negative control. The specificity and cross-reactivities of the antibody raised against the rat PTH/PTHrP receptor were examined using rat kidneys [24] and

Table 1 Scoring system used for the histological appearance of the full-thickness defects of rat articular cartilage

Characteristics	Score
Filling of defects (%)	
125	3
100	4
75	3
50	2
25	1
0	0
Reconstitution of osteochondral junction	
Yes	2
Almost	1
Nonclose	0
Cell morphology	
Normal	4
Mostly hyaline and fibrocartilage	3
Mostly fibrocartilage	2
Some fibrocartilage, but mostly non-chondrocytic cells	1
Non-chondrocytic cell only	0
Matrix staining	
Normal	4
Reduced staining	3
Significant staining	2
Faint staining	1
No staining	0
Perfect score	14

Modified from Pineda et al. [17]

growth plates [25] as a positive control, and rat prostates [26] as a negative control. The specificity and cross-reactivity of the antibody to rat type II collagen was examined using rat articular and growth plate cartilage as a positive control and rat bone as a negative control [27]. For the detection of PCNA, the growth plate of the Wistar rat was used as a positive control. As a negative control, the sections were incubated with either horse or goat serum, or with purified pre-immune mouse or rabbit immunoglobulin G (IgG) (Vector Laboratories, Burlingame, CA, USA) instead of specific antibodies.

For immunostaining of aggrecan, the mouse monoclonal antibody 12/21/1-C-6 was obtained from the Developmental Studies Hybridoma Bank (University of Iowa, Iowa City, IA, USA). Sections were deparaffinized and hydrated. The sections were treated with 0.1 U/ml chondroitinase ABC (Seikagaku Kogyo, Tokyo, Japan) in Tris–acetate buffer pH 8.0 at room temperature for 60 min. Endogenous peroxidase activity was blocked with 0.5% hydrogen peroxide in methanol. The samples were then washed three times in 0.1% BSA in TBS for 5 min, and nonspecific staining was reduced by incubation with horse serum for 30 min. The sections were incubated with a monoclonal antibodies 12/21/1-C-6 (diluted 1:50) overnight at 4°C. A subsequent reaction was performed as described above, and the sections were counterstained with hematoxylin.

In situ hybridization

For in situ hybridization analysis, serial sections (5 μm) of the reparative tissue were prepared at 2, 4, 7, and 10 days, and at 2 and 4 weeks after the creation of smaller full-thickness defects. We first stained the sections with safranin-O, then the semiserial sections were used for in situ hybridization to detect the expression of type II collagen, type X collagen, and PTH/PTHrP receptor mRNA. Sections were deparaffinized in xylene (20 min) and graded ethanol in diethylpyrocarbonate (DEPC)-treated water, followed by two washes in DEPC-treated 0.1 M phosphate buffer (PB) for 1 min each. The slides were then incubated with 10 μg/ml proteinase K (Gibco BRL, Rockville, MO, USA) in 100 mM Tris–HCl and 50 mM EDTA for 30 min at room temperature. The sections were postfixed in 4% PFA for 10 min, followed by one wash with 0.1 M PB. After incubation with 0.2 M HCl, the sections were then washed with 0.1 M PB and 0.1 M triethanolamine (TEA) for 1 min each. The slides were acetylated with acetic anhydride, and after a single wash in 0.1 M PB, dehydrated in ethanol and air-dried. Digoxigenin-labeled cRNA probes were generated by in vitro transcription and labeled with digoxigenin with a DIG RNA labeling kit (Roche, Mannheim, Germany) using the following complementary DNA (cDNA) clones: rat α1(II) collagen cDNA containing a 1.4-kb fragment, mouse α1(X) collagen cDNA containing a 0.65-kb fragment, rat PTH/PTHrP receptor cDNA containing a 2.2-kb fragment, and rat aggrecan cDNA containing a 0.87-kb fragment. The hybridization solution consisted of 50% formamide, 10 mM Tris–HCl, 1× Denhardt's solution, 10% Dextran sulfate, 600 mM NaCl, 0.25% SDS, 1 mM EDTA (pH 8.0), and 200 μg/ml yeast tRNA, into which the probes were diluted. The hybridization mixture was then heated for 3 min at 85°C to denature the probe RNA and then quickly chilled in ice water. The mixture (50 μl) was spread over the pretreated tissue sections, and the sample was then covered with parafilm. Hybridization was performed at 50°C for 16 h. After hybridization and removal of the parafilm by immersion of the slides in 2× SSC for 10 min, the sections were washed in 2× SSC containing 50% formamide. Nonspecific hybridization was removed by 10 μg/ml RNase A in TNE for 30 min at 37°C. After one wash in 2× SSC and two washes in 0.2× SSC at 50°C for 20 min each, hybridization signals were detected immunohistochemically by

alkaline phosphatase-conjugated antibodies using a nucleic acid detection kit (Roche, Mannheim, Germany). Non-specific binding was blocked in a 1% blocking buffer for 60 min at room temperature. The slides were placed in a humid chamber and incubated in ALP-conjugated anti-DIG (1:1,000 dilution) for 45 min at room temperature. The slides were then washed twice with a 1× washing buffer for 20 min each, followed by equilibration in a 1× detection buffer for 5 min. Finally, the sections were stained with a NTB/BCIP solution at room temperature in darkness, for durations varying from 15 min to overnight depending on the mRNA abundancy. After being counterstained with methyl green, the sections were embedded in a crystal mount (Biomeda, Burlingame, USA). The specificity of these cRNA probes was confirmed by the differential distribution of the hybridization signals in the rat growth plate [25, 28].

Statistical analysis

Statistical significance was estimated using the Mann–Whitney's U test. A P value of <0.05 was considered significant.

Results

Histological features during the repair of articular cartilage defects

Using a rat model, we previously established that smaller 0.7 mm V-shaped full-thickness articular cartilage defects spontaneously resurfaced with hyaline cartilage within 4 weeks post-injury [16]. This occurred through the chondrogenic differentiation of mesenchymal cells, which had initially filled the defect cavity. In brief, blood clots were observed at the center of the defect, and spindle-shaped undifferentiated cells were also found to have migrated toward the center of the clot at 2 days after procedure (Fig. 2a). The cavities were mainly filled by spindle-shaped mesenchymal cells at 4 days post-injury, and osteoblastic differentiation was observed adjacent to the residual subchondral bone in depth (Fig. 2b). At 7 days, spindle-shaped undifferentiated cells were present at the surface, and polygonal-shaped cells appeared at the center of the defect (Fig. 2c), where spherical chondrocyte-like cells appeared at 10 days (Fig. 2d). At 2 weeks post-injury, some hypertrophic chondrocyte-like cells were observed adjacent to the newly formed subchondral bone (Fig. 2e). By 4 weeks after their induction, hyaline-like articular cartilage is regenerated concomitantly with the repair of the subchondral bone (Fig. 2f, g). The regenerated articular cartilage exhibited histological characteristics of hyaline cartilage, such as normal morphological characteristics of chondrocytes shown by the appearance of the cells, safranin-O staining of the matrix, and by the vertical columnar arrangement of the chondrocytes. A well-developed, regenerated hyaline articular cartilage persisted at 8 weeks. Diminished matrix staining with safranin-O in this regenerated area was observed from 12 weeks post-injury (data not shown). Thereafter, the regenerated cartilage persisted and maintained its immunoreactivity to type II collagen by 24 weeks (Fig. 2h, i), though the superficial fibrous layer had thickened to some extent.

As shown in Fig. 2, the time course of the cartilage repair process for the smaller 0.7 mm defects was monitored using the histological scoring grades of Pineda, with some modifications (Table 1) [17, 18]. The filling of the defect cavities with fibroblastic undifferentiated cells was the major reparative response of the injured tissue during the first week and had completed by day 7 (with a histological score for the filling of defects of 3.9 ± 0.32). No reconstruction of the osteochondral junction was scored in these cases. However, on the day 7, the initial sign of cartilage formation was histologically scored (the histological score for cell morphology being 0.2 ± 0.82, and a score for matrix staining of 0.1 ± 0.32). Reconstruction of the osteochondral junction was almost completed by the end of the second week post-injury in the smaller defects (histological score 1.7 ± 0.48). The regenerative repair of the cartilage was found to have progressed during the second week (with a histological score for cell morphology of 2.0 ± 0.82, and a score for matrix staining of 1.8 ± 0.79). The regenerative repair of articular cartilage was almost completed by the end of the fourth week (a histological score for cell morphology of 2.8 ± 0.92, and a score for matrix staining of 3.1 ± 0.74), and the histological score was maintained at a high level thereafter (Fig. 2j).

In contrast to the smaller defects, cartilaginous repair responses failed to occur in the larger 1.5 mm defects

Fig. 2 Transverse sections of the smaller 0.7 mm cartilage defects. The distal portion of the rat femur was cut in a transverse plane, and sections were stained with safranin-O at 2 days (**a**), 4 days (**b**), 7 days (**c**), 10 days (**d**), 2 weeks (**e**), 4 weeks (**f**) and 24 weeks (**h**) after the creation of the defects. The specimen sections shown in **f** and **h** were also stained with anti-type II collagen monoclonal antibodies, shown in **g** and **i**, respectively. *Bar* 300 μm. **j** Time course of the histological scores during the repair of the smaller 0.7 mm defects is shown. **k** Schematic diagram of the specimen of the reparative tissue. An *open square* represents the sampling fields used for immunohistochemical and in situ hybridization analyses in Figs. 5, 6, 7, and 8. At the indicated time points after the creation of the defects, the animals were killed to enable histochemical analysis ($n = 10$). Repair responses were monitored using the histological scoring system shown in Table 1 ▶

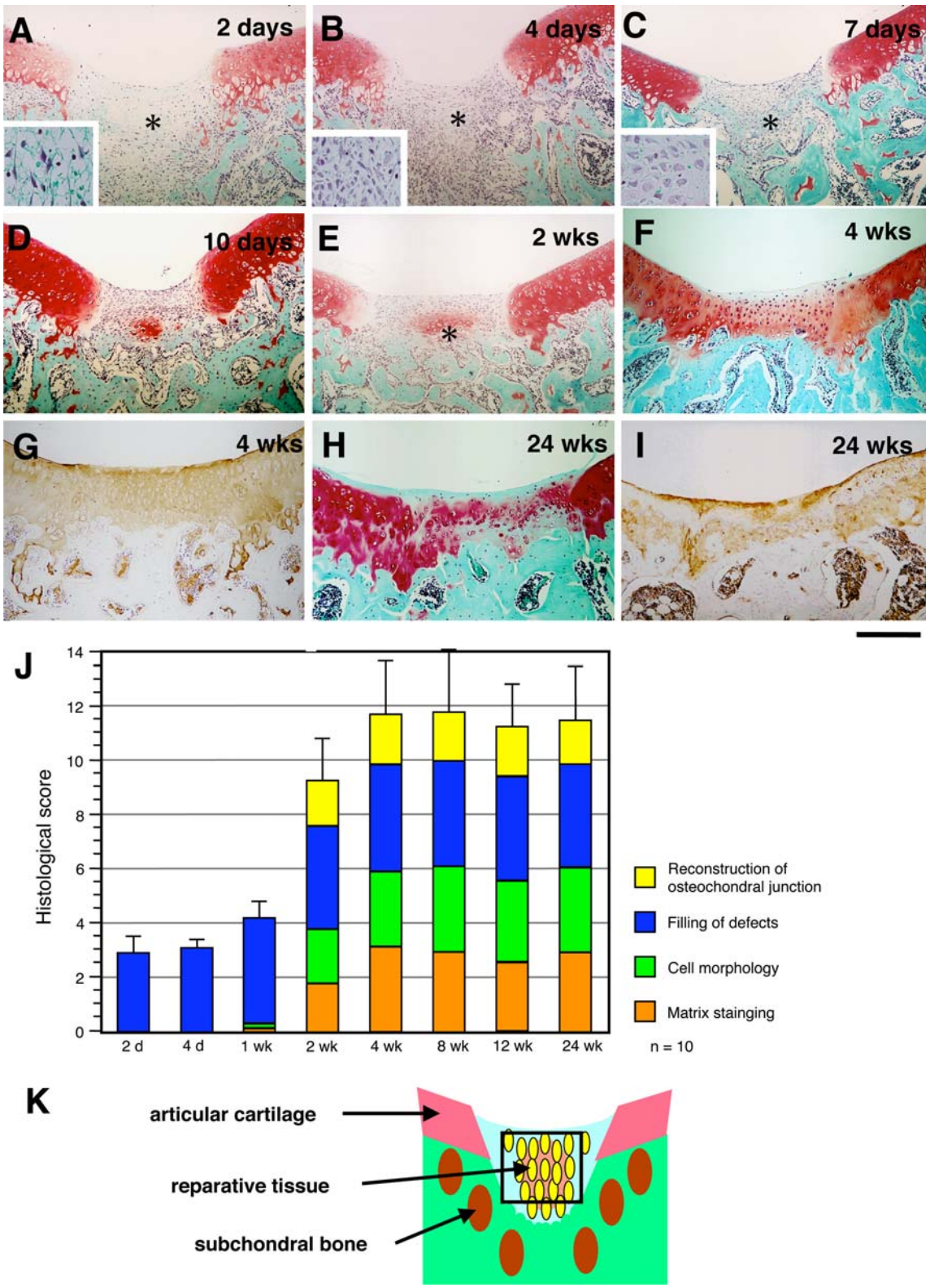

(Fig. 3). At the initial stage of repair (day 2 post-injury), spindle-shaped cells were present at the periphery of the defects at 2 days (Fig. 3a) and many spindle-shaped cells had migrated toward the center of the cavity, and the central area still contained blood clots, by day 4. Osteoblastic differentiation of cells was found to have taken place near the underlying marrow trabeculae (Fig. 3b). Significantly, the migration and filling of the cartilage

cavities with these cells is the only reparative response that could be positively histologically scored during this period for the larger defects (Fig. 3g). The histological scores for the filling of defects on day 2 and 4 were found to be 2.0 ± 0.58 and 2.7 ± 082, respectively. By day 7, the larger defects had almost completely filled with cells (the histological score for filling of defects: 3.4 ± 0.79) in a similar manner to the smaller 0.7 mm defects. Many polygonal-shaped cells were also observed to be present at the periphery of the larger defects, but blood clots remained in the central area at 7 days after their creation (Fig. 3c). However, no reconstruction of the osteochondral junction could be scored at this stage. At 10 days (Fig. 3d) and 2 weeks (Fig. 3e) post-injury, the articular surfaces were found to be covered with fibrous tissue. In addition, the synthesis of woven bone had progressed from the subchondral bone surface and the subchondral bone was almost reconstituted at 4 weeks. However, cells in the reparative tissue areas on the surface of the 1.5 mm defects were mostly non-chondrocytic and the matrix did not stain with safranin-O in these specimens at 4 weeks (Fig. 3f). The histological score for matrix staining reached 0.2 ± 0.41 by week 4, but no further increase in this score was observed for these larger defects, even 8 weeks after the creation of the cavities.

Expression of type II and X collagens, and aggrecan transcripts

The expression of cartilage-type collagens and aggrecan transcripts was examined by in situ hybridization in the reparative tissue of the smaller 0.7 mm defects. Type II and X collagens mRNAs as well as aggrecan mRNA were undetectable at 4 days post-injury in these smaller cavities (data not shown). At 7 days post-injury, however, type II collagen transcripts were detectable in polygonal-shaped cells that had migrated to the center of the defect (Fig. 4a), but type X collagen transcripts were still undetectable (Fig. 4b). Aggrecan mRNA was also detected in polygonal-shaped cells (Fig. 4c). At 2 weeks after the generation of these 0.7 mm cartilage defects, type II collagen mRNA was exclusively detected in chondrocytic cells at the center of the defects (Fig. 4d), and the expression of type X collagen mRNA was found to be restricted to hypertrophic chondrocyte-like cells (Fig. 4e). Chondrocytic cells in the cartilage matrix also expressed aggrecan mRNAs (Fig. 4f). At 4 weeks, most of the chondrocytic cells expressed type II collagen and aggrecan mRNAs at levels that are equivalent to residual articular chondrocytes (Fig. 4g, i). Moreover, type X collagen mRNA was still detectable in hypertrophic chondrocyte-like cells in the deeper layers of the regenerated cartilage, as well as those in the franking intact articular cartilage (Fig. 4h).

Expression of PCNA in the reparative tissue

At 2 days after of the generation of the smaller 0.7 mm rat cartilage defects, immunoreactivity against PCNA was barely evident in the undifferentiated cells that had formed in the cavity (Fig. 5a). At 4 days however, most of these undifferentiated cells stained positively for PCNA (Fig. 5b). At 7 days post-injury, this PCNA immunoreactivity was detectable in the undifferentiated cells beneath the surface area, and in polygonal-shaped cells located in the central region (Fig. 5c). PCNA was also expressed in chondrocyte-like cells and spindle-shaped cells at 2 weeks (Fig. 5d). At 4 weeks, cells in the middle layer of regenerated cartilage were also positively stained with the PCNA antibody, similarly to cells in residual normal articular cartilage (data not shown).

Expression of N-cadherin

The expression of N-cadherin in cells of the reparative tissue in the smaller 0.7 mm defects was also examined by immunohistochemistry. In our preliminary analysis, we assessed the reactivity and specificity of the N-cadherin antibody we used in these experiments, as described in "Materials and methods". The pattern of immunostaining that we observed was very consistent with previous reports [21–23]. At 2 days post-injury, most of the undifferentiated cells in the defects did not express N-cadherin protein (Fig. 6a). In contrast, immunoreactivity was evident in the lining osteoblasts of subchondral bone in the depths of the defect at 2 days post-injury (Fig. 6a, inset). At 4 days, however, N-cadherin was detectable in undifferentiated cells at the center of the defects (Fig. 6b), whereas immunoreactivity against N-cadherin was not observed in cells at the periphery of the defects. At 7 days, the expression of N-cadherin disappeared in the polygonal-shaped cells located in the central region, but was positive in the adjacent spindle-shaped cells (Fig. 6c). From 10 days to 4 weeks (Fig. 6d), the expression of N-cadherin was not evident in the reparative cells except for the osteoblasts lining the subchondral bone surface.

Expression of PTH/PTHrP receptors

We next investigated the expression of the PTH/PTHrP receptors in cells of the reparative tissue in the smaller 0.7 mm defects. Our in situ hybridization analyses revealed that the undifferentiated cells that had migrated to the center of the defects did not express PTH/PTHrP receptor transcripts at 2 days (Fig. 7a). However, at 4 days post-injury, undifferentiated cells at the center of the 0.7 mm cartilage cavities were found to express a high level of PTH/PTHrP receptor mRNA (Fig. 7c). At 7 days, PTH/

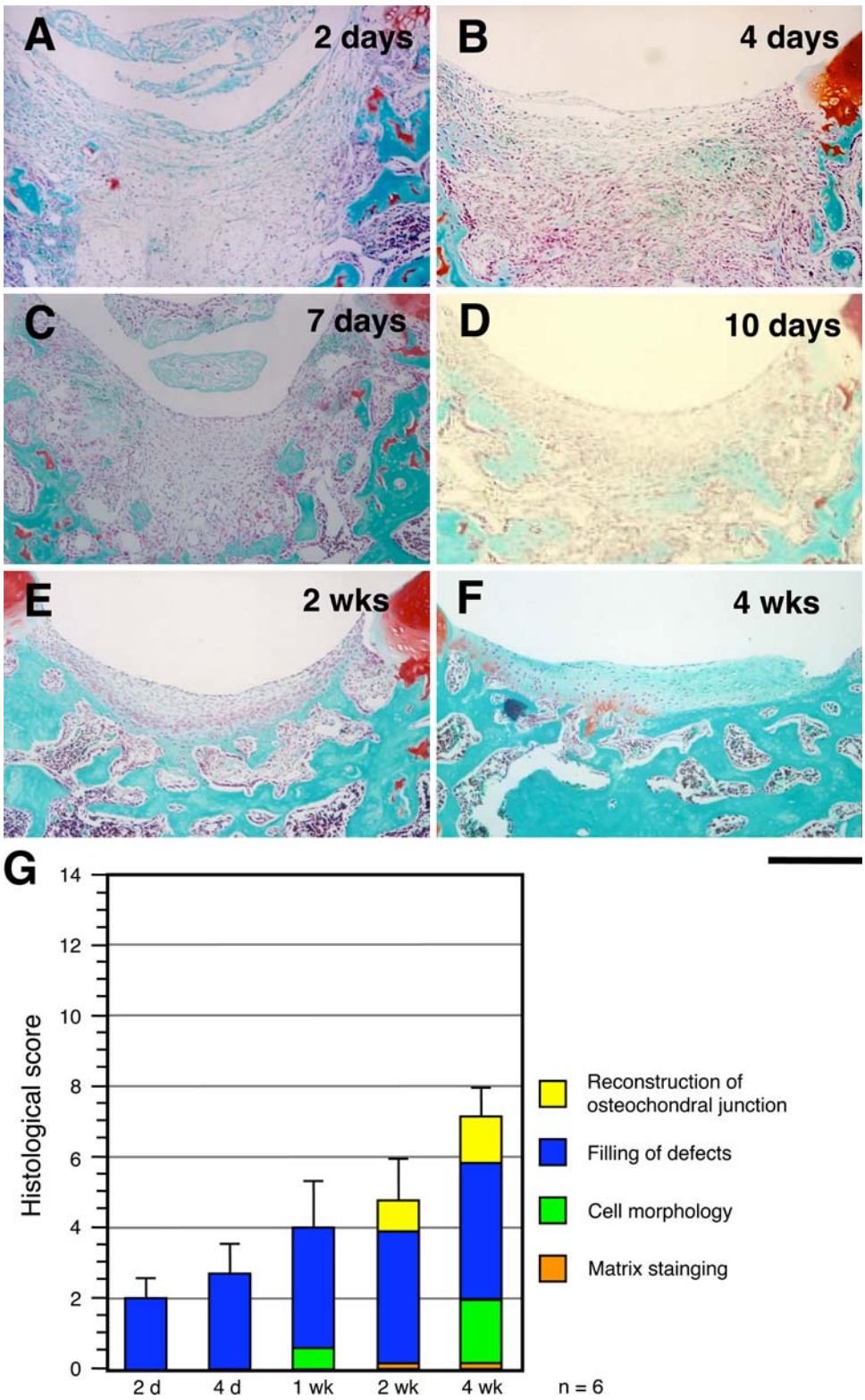

Fig. 3 Transverse sections of the larger 1.5 mm defects. The distal portion of the femur was cut in a transverse plane, and sections were stained with safranin-O at 2 days (**a),** 4 days (**b**), 7 days (**c**) and 10 days (**d),** 2 weeks (**e),** 4 weeks (**f**) after creation of the defects. *Bar* 300 μm. **g** Time course of the histological scores during the repair of the lager 1.5 mm defects is shown. At the indicated time points after the creation of the defects, the animals were killed to enable histochemical analysis ($n = 6$). Repair responses were monitored using the histological scoring system shown in Table 1

PTHrP receptor mRNA was also detectable in the polygonal-shaped cells at the center of the defect and in the superficial undifferentiated cells (Fig. 7e). Thereafter, PTH/PTHrP receptor mRNA was found to be localized in the chondrocyte-like cells (data not shown).

As a preliminary experiment, we tested the reactivity and specificity of our PTH/PTHrP receptor protein antibody in rat tissues and the pattern of immunostaining accorded well with previous reports [24–26]. The immunoreactivity of the PTH/PTHrP receptor in undifferentiated

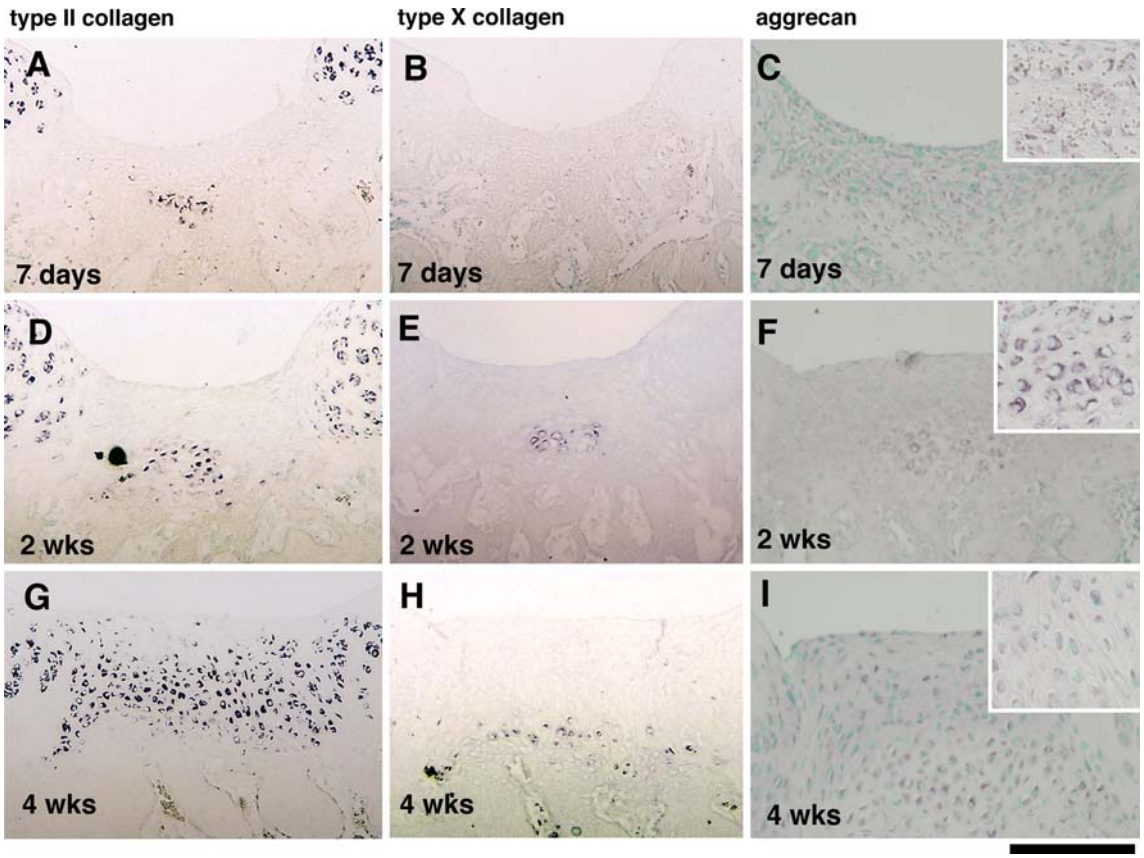

Fig. 4 In situ hybridization of type II, X collagen and aggrecan mRNAs in the smaller 0.7 mm defects at 7 days (**a**–**c**), 2 weeks (**d**–**f**), and 4 weeks (**g**–**i**) post-injury. **a**, **d**, **g** The expression of type II collagen mRNA, **b**, **e**, **h** the expression of type X collagen mRNA. **c**, **f**, **i** The expression of aggrecan mRNA. The *inset* of **c**, **f**, and **i** shows the aggrecan positive polygonal-shaped cells (**c**) and chondrocyte-like cells (**f**, **i**). Sections were counterstained with Methyl Green. *Bar* 300 μm

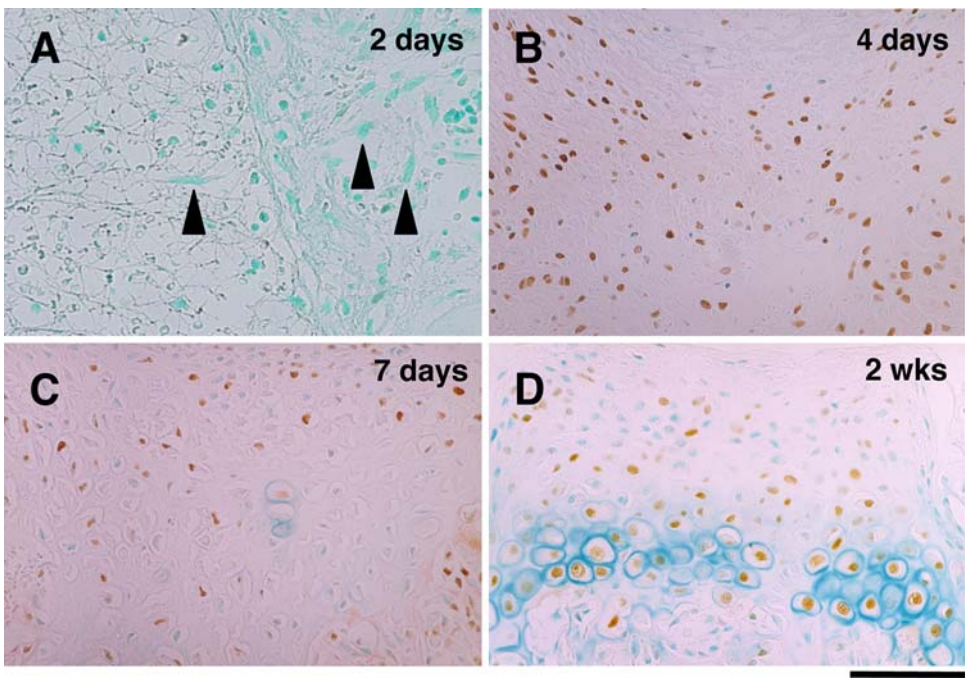

Fig. 5 Expression of PCNA during the early phases of the repair process in the smaller 0.7 mm defects at 2 days (**a**), 4 days (**b**), 7 days (**c**), and 2 weeks (**d**) post-injury. **a**–**d** The PCNA-positive cells in the corresponding areas denoted by *asterisks* in **a**–**c**, and **e** and illustration in Fig. 2. *Arrowheads* in **a** indicate spindle-shaped cells. Sections were counterstained with Methyl Green. *Bar* 100 μm

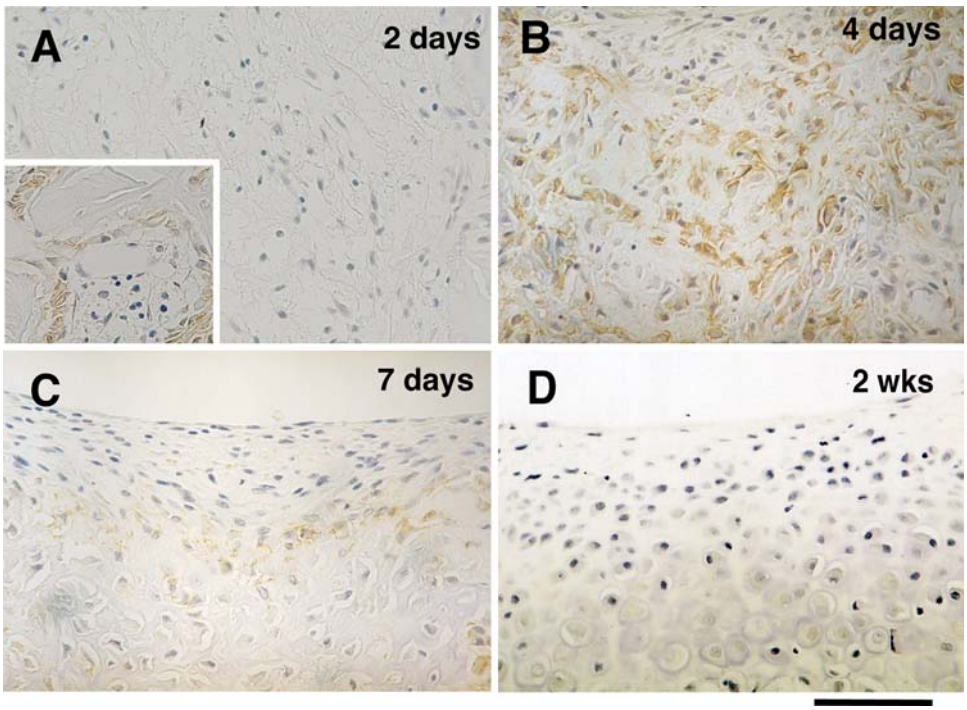

Fig. 6 Expression of N-cadherin during the early phase repair process in the smaller 0.7 mm full-thickness defects at 2 days (**a**), 4 days (**b**), 7 days (**c**) and 2 weeks (**d**) post-injury. **a–d** The expression of N-cadherin proteins in the corresponding areas denoted by the *asterisks* in **a–c** and **e** and illustration in Fig. 2. The *inset* of **a** shows immunoreactivity of the osteoblasts lining the subchondral bone. Sections were counterstained with hematoxylin. *Bar* 100 μm

cells that had migrated to the center of the smaller defects was rarely evident at 2 days (Fig. 7b). At 4 days however, PTH/PTHrP receptor immunoreactivity was detectable in most of the undifferentiated cells that filled the whole cavity (Fig. 7d). At 7 days, PTH/PTHrP receptor immunoreactivity was also evident in the type II collagen positive polygonal-shaped cells (Fig. 7f). At 4 weeks, the PTH/PTHrP receptor was widely immunostained in the differentiated chondrocytes in the reparative tissue (data not shown). Hence, the pattern of the immunolocalization of the PTH/PTHrP receptor proteins was consistent with that of its mRNA.

Expression of Sox9

The expression of Sox9 in cells of the reparative tissue in the smaller 0.7 mm defects was also examined by immunohistochemistry. The immunoreactivity of the Sox9 in undifferentiated cells that had migrated to the center of the smaller defects was rarely evident at 2 days (Fig. 8a). However, at 4 days post-injury, undifferentiated cells at the center of the 0.7 mm cartilage cavities were found to express Sox9 protein (Fig. 8c). At 7 days, Sox9 protein was also detectable in the polygonal-shaped cells at the center of the defect and in the superficial undifferentiated cells (Fig. 8e). Immunoreactivity for Sox9 protein was found in chondrocyte-like cells, whereas it was rarely detected in hypertrophic chondrocytes in the deep zone (Fig. 8g).

Expression of Runx2

The expression of Runx2 was examined by immunohistochemistry in the reparative tissue of the smaller 0.7 mm defects. Immunoreactivity of Runx2 in the reparative tissues was not observed by 7 days post-injury in these cavities (Fig. 8b, d, and f). Two weeks after the generation of defects, the expression of Runx2 protein was found to be restricted to hypertrophic chondrocyte-like cells (Fig. 8h). At 4 weeks, Runx2 protein was still detectable in hypertrophic chondrocyte-like cells in the deeper layers of the regenerated cartilage, as well as those in the franking intact articular cartilage (data not shown).

Discussion

Experimental animal studies indicate that smaller full-thickness defects can undergo regenerative repair under the limited condition, whereas larger defects heal less well [1, 3, 5]. Among animal species, there are differences in the threshold sizes of the defects at which chondrogenic repair response are induced [1, 3, 6]. We previously reported that full-thickness cylindrical defects of small (3 mm) size created in the femoral trochlea of adolescent rabbits showed complete regenerative repair of the damaged cartilage within 8 weeks, whereas chondrogenic repair response does not occur in the large (5 mm) diameter full-thickness defects. In our current experiments,

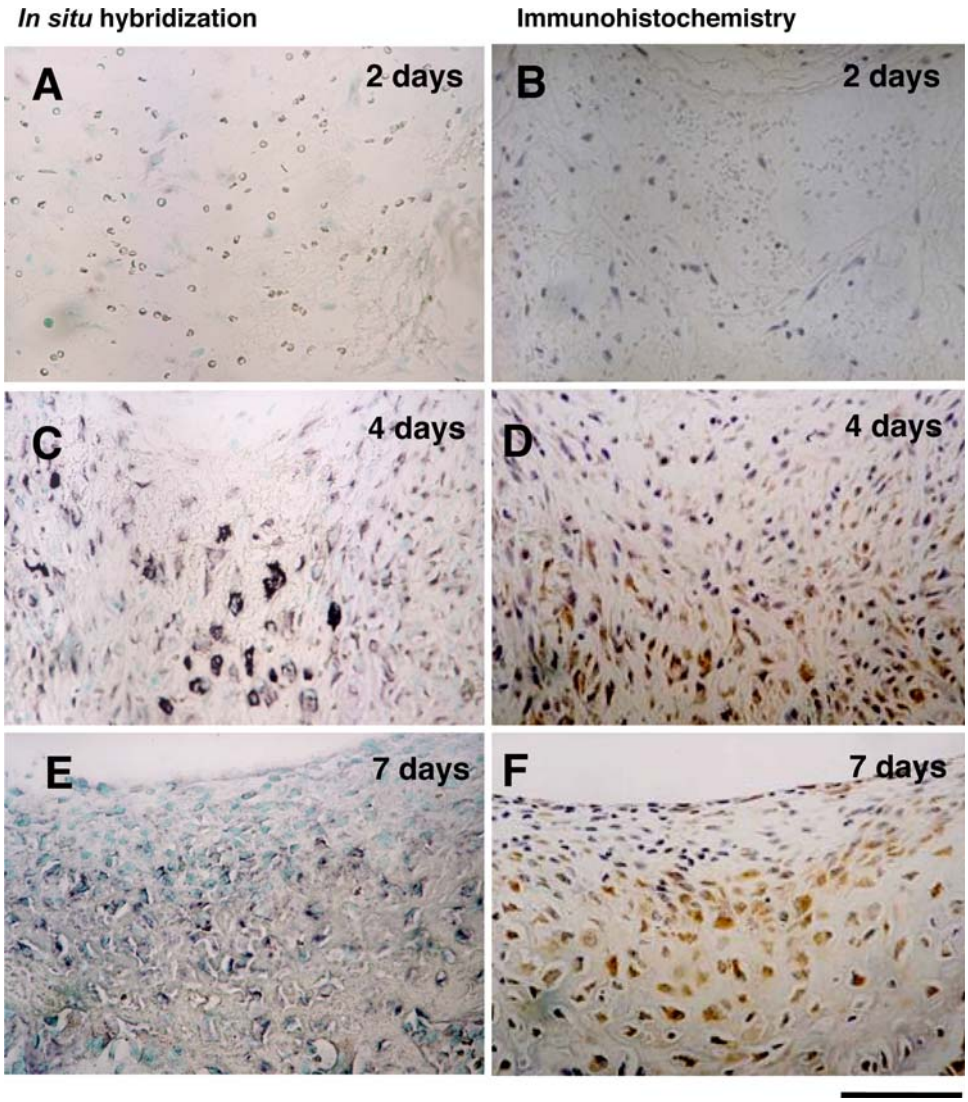

Fig. 7 Expression of PTH/PTHrP receptor mRNA and protein during the early phases of the cartilage repair process in the smaller 0.7 mm defects. The defects at 2 days (**a**, **b**), 4 days (**c**, **d**), and 7 days (**e**, **f**) after their generation are shown. **a**, **c**, **e** In situ hybridization of PTH/PTHrP receptor mRNA in the corresponding areas denoted by the *asterisks* in **a**–**c** in Fig. 2. **b**, **d**, **f** Immunolocalization of PTH/PTHrP receptor protein in the corresponding areas denoted by *asterisks* in **a**–**c** and illustration in Fig. 2. Sections were counterstained with Methyl Green (**a**, **c**, **e**) or hematoxylin (**b**, **d**, **f**). *Bar* 100 μm

histochemical analysis showed that the smaller V-shaped 0.7 mm defects created with this device spontaneously regenerated the surfacing rat articular cartilage in a precise temporal sequence (Figs. 2, 4). The defect cavities were filled with undifferentiated cells at 4 days after their creation, followed by the appearance of type II collagen-expressing cells at the center of these cavities by day 7 (Figs. 2, 4). Type X collagen-expressing hypertrophic cells appeared in the depths of the cavities from 2 weeks post-injury. Moreover, as hyaline cartilage expanded in the cavities, the structure of the surfacing articular cartilage was found to have regenerated concomitantly with the repair of the subchondral bone within 4 weeks (Figs. 2, 4). In contrast, the larger 1.5 mm defects failed to regenerate surfacing cartilage and were covered only with fibrous scar tissue (Fig. 3). Our rat model of articular cartilage repair proceeds in a manner that is dependent on the size of the defects.

We previously found in our rabbit model of full-thickness defects of articular cartilage that the mobilization and accumulation of proliferative mesenchymal cells into the defect cavities correlated well with the capacity to subsequently induce of cartilaginous repair [10, 11]. A previous in vitro model of chondrogenesis also supports the notion that undifferentiated mesenchymal progenitors are in a highly proliferative state prior to overt chondrogenesis [29, 30]. In our rabbit model, we earlier demonstrated that both endogenous and exogenous FGF-2 (fibroblast growth factor-2) plays a pivotal role during the active migration of undifferentiated mesenchymal cells at the early defect-filling stage of cartilaginous repair [8, 10]. By taking advantage of our new rat model system, we analyzed such early stages of regenerative repair of articular cartilage in our current study. In rat 0.7 mm defects, as shown in Fig. 2a, spindle-shaped undifferentiated cells had already begun to migrate toward the center of the cavities and had

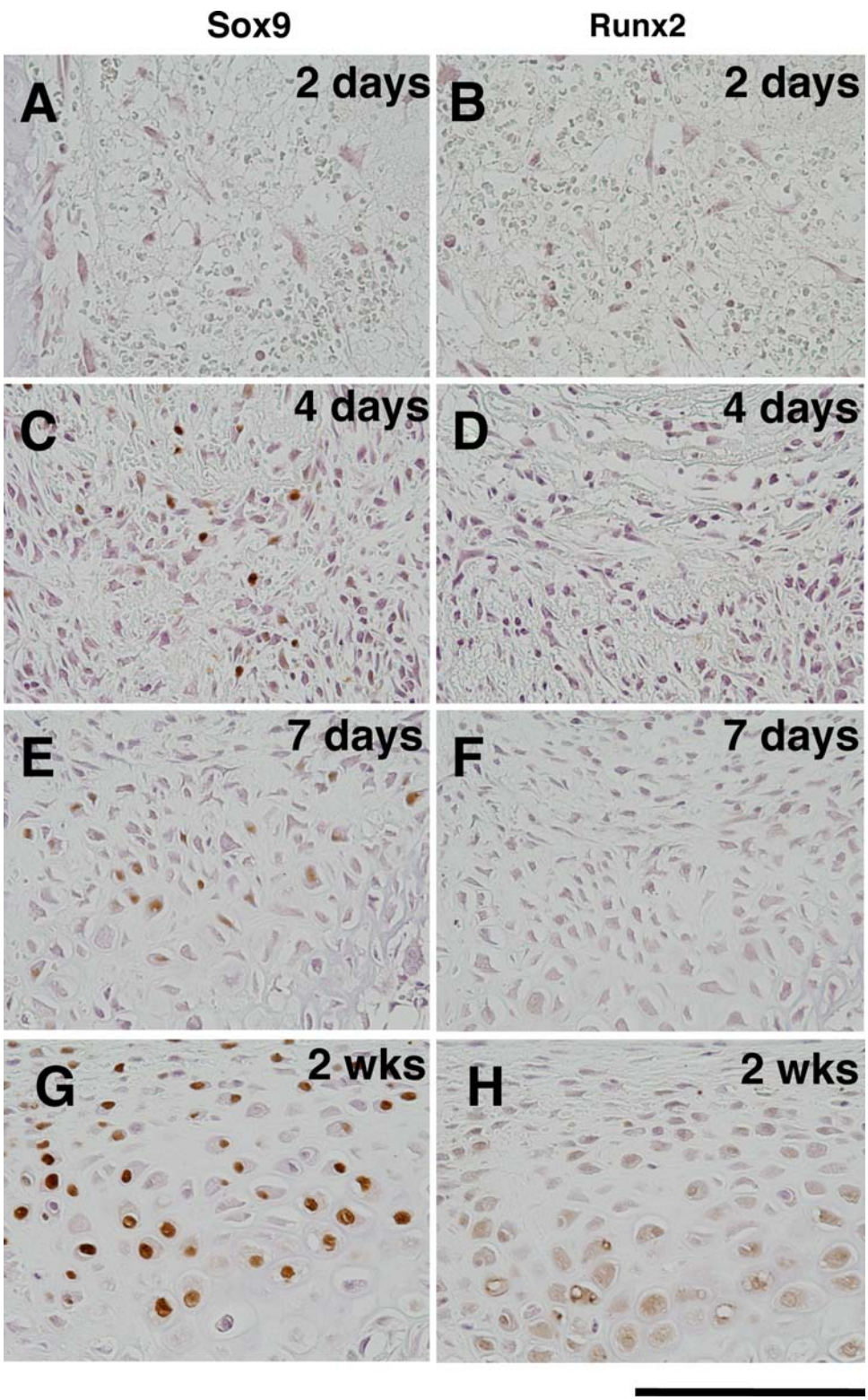

Fig. 8 Expression of Sox9 and Runx2 protein during the early phases of the cartilage repair process in the smaller 0.7 mm defects. The defects at 2 days (**a**, **b**), 4 days (**c**, **d**), 7 days (**e**, **f**), 2 weeks (**g**, **h**) after their generation are shown. **a**, **c**, **e**, **g** Sox9 protein in the corresponding areas denoted by the *asterisks* in **a**–**c** and **e** and illustration in Fig. 2. **b**, **d**, **f** Immunolocalization of Runx2 protein in the corresponding areas denoted by *asterisks* in **a**–**c** and **e** and illustration in Fig. 2. Sections were counterstained with hematoxylin. *Bar* 100 μm

almost filled the defect within the first 2 days post-injury. Although some PCNA-positive cells were found at the periphery of subchondral bone in the depths of the defect, most cells filling the center of the cavities were PCNA-negative at this early stage (Fig. 5). However, as indexed by a high incidence of PCNA-positive cells, most undifferentiated cells in the defects were in a highly proliferative state prior to cartilage formation by day 4 (Fig. 5). Thus, prior to the acquisition of proliferative activity, bone marrow-derived undifferentiated cells rapidly migrate and

fill the defect cavities. It is also quite probable that FGF-2 plays a role at this very early stage of repair [10].

PTH/PTHrP receptor signaling slows down the progression of chondrogenic differentiation of cells during embryonic development [30–32]. In vitro studies have also revealed that the expression of the PTH/PTHrP receptor is induced by the commitment to the chondrogenic differentiation of mesenchymal progenitors at the cellular condensation stage [30, 34]. In our previous study using a rabbit model [18], we reported that the chondrogenic capacity of cells that had migrated to the defect cavities was closely associated with their expression of the PTH/PTHrP receptor. In line with this observation, PTH/PTHrP receptor was found in our present analyses to be expressed in cells that had migrated and filled the rat cartilage defect cavities by day 4 post-injury (Fig. 7). It is noteworthy here that no PTH/PTHrP receptor expression was detectable in cells that filled the defects during the initial stages of repair at day 2. Thus, these cells acquire the responsiveness to PTH/PTHrP signals after their migration into the defects between day 2 and 4.

Cellular condensation is a prerequisite for the initiation of chondrogenesis, both in the embryonic limb bud and in mesenchymal cell cultures [35, 40]. In the limb bud region, a shift of collagen expression from type I to type II occurs, and thereafter chondrocytes acquire a characteristic round cell morphology and synthesize cartilage extracellular matrix [41, 42]. Among others, N-cadherin is a well-known molecule that appears on the surface of mesenchymal cells prior to the onset of overt chondrogenesis and participates in the cell–cell interaction during mesenchymal condensation [43–46]. The expression of N-cadherin is highest in undifferentiated mesenchymal cells at the cellular condensation phase, and then decreases as differentiation progresses [43, 46]. No N-cadherin is detectable in mature chondrocytes. Oberlender et al. demonstrated in an earlier study that a significant inhibition of chick limb bud mesenchymal condensation in vitro and in vivo occurs with the use of a function-blocking monoclonal antibody, NCD-2, which is directed against N-cadherin [43]. As shown in Figs. 5 and 6 in this study, immunohistochemistry reveals that the N-cadherin expression prevails at the central point of the defects within the PCNA-positive cell population at day 4. Overlapping this central point, type II collagen expressing polygonal-shaped cells are subsequently generated by day 7, although N-cadherin immunoreactivity had already been lost from these cells by this time. Hence, prior to cartilage formation, migrated cells in the reparative tissue undergo a commitment to chondrogenesis via a differentiation step that is equivalent to mesenchymal condensation.

In the present study, immunohistochemical studies were carried out with polyclonal antibodies against Sox9 and Runx2, which are important transcription factors for chondrogenesis. Sox9 is prerequisite for transcription of *Col2a1* gene and the maintenance of chondrocyte phenotype [36, 37]. Runx2 is required for osteoblast differentiation, and also regulates chondrocyte maturation and terminal differentiation during skeletogenesis [38, 39]. During the repair of 0.7 mm smaller full-thickness articular cartilage defects, the expression of Sox9 was induced at 4 days after creation of the defects before type II collagen synthesis became apparent. Thereafter immunoreactivity for Sox9 was continuously expressed in the repair chondrocytes. Hypertrophic chondrocytes appeared at 2 weeks, and Runx2 protein was expressed in these hypertrophic chondrocytes at the depth of the newly formed cartilage. In contrast, immunoreactivity for Sox9 was rarely detected in the hypertrophic chondrocytes. These results suggest that Sox9 is also involved in the induction of chondrogenic repair response, and the reduced expression of Sox9 in combination with induction of Runx2 expression is important for the cartilage maturation and subsequent calcification in the regenerative repair of articular cartilage.

In summary, our present analyses have yielded the following findings: (1) Marrow-derived mesenchymal cells acquire higher levels of proliferative activity in the rat cartilage defect cavities after their initial migration stage and fill the defects; and (2) Following migration and filling of the cartilage defects, a distinctive step occurs that is analogous to precartilaginous condensation that is pivotal during chondrogenesis. Rats have several advantages over rabbits that include low costs, availability, and relative ease of handling. Further investigations of the utility of certain growth factors in articular cartilage repair are now underway by using our rat models. These will provide novel insights into possible new therapeutic approaches for cartilage regeneration.

Acknowledgments This work was supported in part by the Grants-in-aid from the Ministry of Education, Culture, Sports, Science, and Technology of Japan. The monoclonal antibody developed by Bruce Carterson was obtained from Developmental Studies Hybridoma Bank developed under the auspices of the NICHD and maintained by The University of Iowa, Department of Biological Sciences, Iowa City.

References

1. Buckwalter J, Rosenberg L, Coutts R, Hunziker E, Reddi AH, Mow V (1988) Articular cartilage: injury and repair of the musculoskeletal soft tissues. In: Woo SL-Y, Buckwalter JA (eds) American Academy of Orthopaedic Surgeons. Park Ridge, pp 465–482
2. Hunziker EB, Rosenberg LC (1996) Repair of partial-thickness defects in articular cartilage: cell recruitment from the synovial membrane. J Bone Joint Surg Am 78:721–733
3. Convery F, Akeson W, Koewn G (1972) The repair of osteochondral defects: an experimental study in horses. Clin Orthop 82:253–262

4. Kim HK, Moran ME, Salter RB (1991) The potential for regeneration of articular cartilage in defects created by chondral shaving and subchondral abrasion. An experimental investigation in rabbits. J Bone Joint Surg Am 73:1301–1315
5. Shapiro F, Koide S, Glimcher MJ (1993) Cell origin and differentiation in the repair of full-thickness defects of articular cartilage. J Bone Joint Surg Am 75:532–553
6. DePalma AF, McKeever CD, Subin DK (1966) Process of repair of articular cartilage demonstrated by histology and autoradiography with tritiated thymidine. Clin Orthop 48:229–242
7. Solchaga LA, Goldberg VM, Caplan AI (2001) Cartilage regeneration using principles of tissue engineering. Clin Orthop Relat Res 391 Suppl:S161–S170
8. Otsuka Y, Mizuta H, Takagi K, Iyama K, Yoshitake Y, Nishikawa K, Suzuki F, Hiraki Y (1997) Requirement of fibroblast growth factor signaling for regeneration of epiphyseal morphology in rabbit full-thickness defects of articular cartilage. Dev Growth Differ 39:143–156
9. Kudo S, Mizuta H, Otsuka Y, Takagi K, Hiraki Y (2000) Inhibition of chondrogenesis by parathyroid hormone in vivo during repair of full-thickness defects of articular cartilage. J Bone Miner Res 15:253–260
10. Chuma H, Mizuta H, Kudo S, Takagi K, Hiraki Y (2004) One day exposure to FGF-2 was sufficient for the regenerative repair of full-thickness defects of articular cartilage in rabbits. Osteoarthritis Cartilage 12:834–842
11. Mizuta H, Kudo S, Nakamura E, Otsuka Y, Takagi K, Hiraki Y (2004) Active proliferation of mesenchymal cells prior to the chondrogenic repair response in rabbit full-thickness defects of articular cartilage. Osteoarthritis Cartilage 12:586–596
12. Noguchi T, Oka M, Fujino M, Neo M, Yamamuro T (1994) Repair of osteochondral defects with grafts of cultured chondrocytes. Comparison of allografts and isografts. Clin Orthop Relat Res 312:251–258
13. Grundnes O, Reikeras O (1995) Effects of function and weight-bearing on the healing of full-thickness cartilage defects in rats. Scand J Med Sci Sports 5:297–301
14. Nishimori M, Deie M, Kanaya A, Exham H, Adachi N, Ochi M (2006) Repair of chronic osteochondral defects in rat. A bone marrow-stimulating procedure enhanced by cultured allogenic bone marrow mesenchymal stroma cells. J Bone Joint Surg Br 88(9):1236–1244
15. Yoshioka M, Kubo T, Coutts RD, Hirasawa Y (1998) Differences in the repair process of longitudinal and transverse injuries of cartilage in the rat knee. Osteoarthritis Cartilage 6:66–75
16. Anraku Y, Mizuta H, Sei A, Kudo S, Nakamura E, Senba K, Takagi K, Hiraki Y (2008) The chondrogenic repair response of undifferentiated mesenchymal cells in rat full-thickness articular cartilage defects. Osteoarthritis Cartilage 16(8):961–964
17. Pineda S, Pollack A, Stevenson S, Goldberg V, Caplan A (1992) A semiquantitative scale for histologic grading of articular cartilage repair. Acta Anat Basel 143:335–340
18. Mizuta H, Kudo S, Nakamura E, Takagi K, Hiraki Y (2006) Expression of the PTH/PTHrP receptor in chondrogenic cells during the repair of full-thickness defects of articular cartilage. Osteoarthritis Cartilage 14:944–952
19. Fujii T, Ueno T, Kagawa T, Sugawara T, Yamamoto T (2005) Immunohistochemical analysis of Sox-9 expression in periosteum of tibia and calvaria after surgical release of periosteum. Acta Histochem 106(6):427–437
20. Tang GH, Rabie AB (2005) Runx2 regulates endochondral ossification in condyle during mandibular advancement. J Dent Res 84(2):166–171
21. Ferrari SL, Traianedes K, Thorne M, Lafage-Proust MH, Genever P, Cecchini MG, Behar V, Bisello A, Chorev M, Rosenblatt M, Suva LJ (2000) A role for N-cadherin in the development of the differentiated osteoblastic phenotype. J Bone Miner Res 15:198–208
22. Schulze C, Firth JA (1993) Immunohistochemical localization of adherens junction components in blood-brain barrier microvessels of the rat. J Cell Sci 104(Pt 3):773–782
23. Lagunowich LA, Donoso LA, Grunwald GB (1990) Identification of mammalian and invertebrate analogues of the avian calcium-dependent cell adhesion protein N-cadherin with synthetic-peptide directed antibodies against a conserved cytoplasmic domain. Biochem Biophys Res Commun 172:313–320
24. Amizuka N, Lee HS, Kwan MY, Arazani A, Warshawsky H, Hendy GN, Ozawa H, White JH, Goltzman D (1997) Cell-specific expression of the parathyroid hormone (PTH)/PTH-related peptide receptor gene in kidney from kidney-specific and ubiquitous promoters. Endocrinology 138:469–481
25. van der Eerden BC, Karperien M, Gevers EF, Lowik CW, Wit JM (2000) Expression of Indian hedgehog, parathyroid hormone-related protein, and their receptors in the postnatal growth plate of the rat: evidence for a locally acting growth restraining feedback loop after birth. J Bone Miner Res 15:1045–1055
26. Urena P, Kong XF, Abou-Samra AB, Juppner H, Kronenberg HM, Potts JT Jr, Segre GV (1993) Parathyroid hormone (PTH)/PTH-related peptide receptor messenger ribonucleic acids are widely distributed in rat tissues. Endocrinology 133:617–623
27. Scheven BA, Hamilton NJ, Farquharson C, Rucklidge GJ, Robins SP (1988) Immunohistochemical localization of native and denatured collagen types I and II in fetal and adult rat long bones. Bone 9:407–414
28. Alvarez J, Balbin M, Santos F, Fernandez M, Ferrando S, Lopez JM (2000) Different bone growth rates are associated with changes in the expression pattern of types II and X collagens and collagenase 3 in proximal growth plates of the rat tibia. J Bone Miner Res 15:82–94
29. George M, Chepenik KP, Schneiderman MH (1983) Proliferation of cells undergoing chondrogenesis in vitro. Differentiation 24:245–249
30. Shukunami C, Shigeno C, Atsumi T, Ishizeki K, Suzuki F, Hiraki Y (1996) Chondrogenic differentiation of clonal mouse embryonic cell line ATDC5 in vitro: differentiation-dependent gene expression of parathyroid hormone (PTH)/PTH-related peptide receptor. J Cell Biol 133:457–468
31. Lanske B, Karaplis AC, Lee K, Luz A, Vortkamp A, Pirro A, Karperien M, Defize LH, Ho C, Mulligan RC, Abou-Samra AB, Juppner H, Segre GV, Kronenberg HM (1996) PTH/PTHrP receptor in early development and Indian hedgehog-regulated bone growth. Science 273:663–666
32. Chung UI, Lanske B, Lee K, Li E, Kronenberg H (1998) The parathyroid hormone/parathyroid hormone-related peptide receptor coordinates endochondral bone development by directly controlling chondrocyte differentiation. Proc Natl Acad Sci USA 95:13030–13035
33. Huang W, Chung UI, Kronenberg HM, de Crombrugghe B (2001) The chondrogenic transcription factor Sox9 is a target of signaling by the parathyroid hormone-related peptide in the growth plate of endochondral bones. Proc Natl Acad Sci USA 98:160–165
34. Shukunami C, Ohta Y, Sakuda M, Hiraki Y (1998) Sequential progression of the differentiation program by bone morphogenetic protein-2 in chondrogenic cell line ATDC5. Exp Cell Res 241:1–11
35. Ede DA (1983) Cellular condensations and chondrogenesis. In: Hall BK (ed) Cartilage, vol 2. Academic Press, New York, pp 143–185
36. Lefebvre V, Huang W, Harly VR, Goodfellow PN, de crombrugghe B (1997) Sox-9 is a potent activator of the chondrocyte-

specific enhancer of the proa1(II) collagen gene. Mol Cell Biol 17:2336–2346
37. Ng LJ, Wheatly S, Muscat GE, Conway-Campbell J, Bowles J, Wright E et al (1997) Sox9 binds DNA, activates transcription, and coexpression with type II collagen during chondrogenesis in the mouse. Dev Biol 183:108–121
38. Ducy P, Zang R, Geoffroy V, Ridall AL, Karsenty G (1997) Osf2/Cbfa1: a transcriptional activator of osteoblast differentiation. Cell 89:747–754
39. Inada M, Yasui T, Nomura S, Deguchi K, Himeno M et al (1999) Maturational disturbance of chondrocytes in cbfa1-deficient mice. Dev Dyn 214:279–290
40. Hall BK, Miyake T (2000) All for one and one for all: condensations and the initiation of skeletal development. Bioessays 22:138–147
41. Nah HD, Rodgers BJ, Kulyk WM, Kream BE, Kosher RA, Upholt WB (1988) In situ hybridization analysis of the expression of the type II collagen gene in the developing chicken limb bud. Coll Relat Res 8:277–294
42. DeLise AM, Fischer L, Tuan RS (2000) Cellular interactions and signaling in cartilage development. Osteoarthritis Cartilage 8:309–334
43. Oberlender SA, Tuan RS (1994) Expression and functional involvement of N-cadherin in embryonic limb chondrogenesis. Development 120:177–187
44. Haas AR, Tuan RS (1999) Chondrogenic differentiation of murine C3H10T1/2 multipotential mesenchymal cells: II. Stimulation by bone morphogenetic protein-2 requires modulation of N-cadherin expression and function. Differentiation 64:77–89
45. Tufan AC, Tuan RS (2001) Wnt regulation of limb mesenchymal chondrogenesis is accompanied by altered N-cadherin-related functions. FASEB J 15:1436–1438
46. Kawai J, Akiyama H, Shigeno C, Ito H, Konishi J, Nakamura T (1999) Effects of transforming growth factor-beta signaling on chondrogenesis in mouse chondrogenic EC cells, ATDC5. Eur J Cell Biol 78:707–714